# The Recovery of Waste Polypropylene & Synthesis of a Sustainable Extrudable Paste for Additive Manufacturing

*Amanda Siciliano, Bryson Clifford, Devorah Cahn, Benjamin Hude-Velasco*

## Objectives

In December 2019, the respiratory infection COVID-19 was declared a pandemic by the World Health Organization (WHO). In the subsequent governmental responses worldwide, the use of single-use masks became widespread as a key component in limiting the spread of the causatory virus. While these masks have long been used within the medical industry, with the institution of mask mandates in many countries, the demand for these single-use masks was estimated to rise to approximately 129 billion masks worldwide per month (Prata 2020). While many of these masks will be incinerated due to their biohazard nature, many more will be processed by conventional waste disposal methods and contribute to global plastic pollution—already a large environmental concern with an estimated 4.8-10 million metric tonnes of plastic waste entering the ocean in 2010 (Jambeck 2015).

While still a small segment of the overall industry, Additive Manufacturing (AM) was still estimated to be worth ~$10 billion in 2019 and continued to grow during 2020, despite the impact of the Coronavirus pandemic (AMFG). Applications using polymers are some of the most common, driven in part due to the recent emergence of high-performance materials: from 2019 to 2020, the Senvol Database (a database of industrial AM machines and materials) grew from just over 1,700 materials to just over 2,245 different AM materials (AMFG). As the industry continues to grow, a key aspect of that growth will be the development of new materials that allow AM to expand into new markets.

This project looks to address both issues concurrently. One of the primary components of the single-use masks is polypropylene, a high-performance commercial polymer, exactly the type of material needed by additive manufacturing. Used face masks then become a resource rather than a waste. Thus this project comprises two primary aims:

- **Aim 1:** *Recover* polypropylene (PP) from Covid-19 face mask waste using selective solvent-recovery techniques
- **Aim 2:** Use the recovered PP to *synthesize* a more sustainable extrudable polymer filament for additive manufacturing

By exploring how these aims may be achieved, polymer physics concepts such as crystalline structure, phase separation, and cohesive energy density will be explored.

## Introduction

### *Polypropylene: Manufacturing and Properties*

In an effort to stop the spread of the coronavirus disease during the ongoing global pandemic, WHO issued guidelines advising the use of face masks (CDC 2020). These face masks are required to be worn in public settings, events and gatherings, and other areas that run the risk of human interaction. Face masks are designed to stop the spread of COVID-19 by entirely

covering the nose and mouth regions through multiple layers of breathable fabric. Although certain medical professionals and emergency responders are required to wear other personal protective equipment (PPE), including gloves, gowns, and face shields, face masks continue to be the most popular type of PPE used by the general public. As a result, the N95 masks and disposable surgical masks are the most popular types of face coverings used in the COVID-19 pandemic. These masks typically come with three layers consisting of an inner layer, a filter, and an outer layer. The inner layer tends to be made of hydrophilic materials, such as cotton, that can absorb water droplets from a person's breath or cough. The filter and outer layers tend to be made of hydrophobic materials, such as polypropylene and polyester, that can repeal these potentially infectious water droplets. Although these face coverings have been instrumental in stopping the spread of the coronavirus, research indicates that their increased usage has been detrimental to the environment due to the increased plastic pollution. In fact, plastic waste has increased beyond just PPE materials, as once banned single-use plastics, such as grocery bags and takeout containers, have now been permitted in an attempt to avoid cross-contamination and disease spread (Patrício Silva et al. 2020). The insurmountable plastic waste that will result from the COVID-19 pandemic generates the need for better methods of managing medical and plastic waste. If better strategies are not created, there will be serious environmental concerns over microplastic pollution. One promising solution lies in the recycling and recovery of polypropylene from face masks. Research indicates that N95 masks have about 11 grams of polypropylene while disposable surgical masks have about 4.5 grams of polypropylene (Akber Abbasi 2020). By analyzing the fundamental properties of nonwoven fabrics like polypropylene, it is possible to develop a research plan for the recovery and recycling of waste plastic from COVID-19 face masks.

While there are multiple sources of plastic within the different layers of the disposable surgical face masks, this research focuses specifically on repurposing the polypropylene filter layer. Further examination of this filter layer reveals that it is made of a nonwoven melt-blown polypropylene material. Nonwovens are fabrics made through the bonding of mass fibers through various heat, chemical, or mechanical means. As a result, these fibers have very high tensile strength and durability, making them favorable for face covering applications where mobility and structural integrity is crucial. The two main processes for making nonwovens include spunbond and meltblown. In both processes, as shown in **Figure 1.0**, raw polymeric filament materials pass through various stages including a resin feed system, extruder assembly, metering pump, collector and winder unit (Edwards 2020, Hutten 2007).

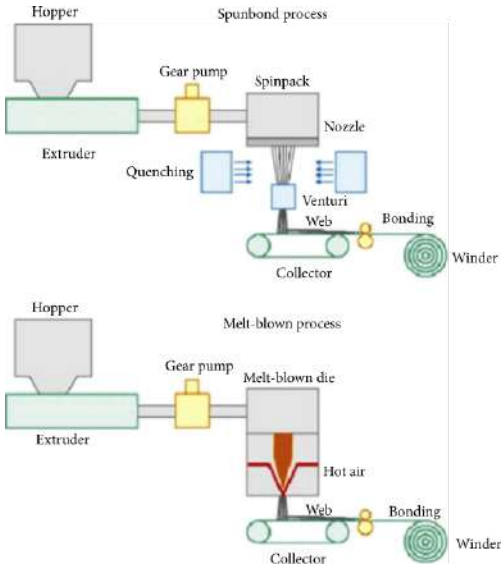


**Figure 1:** Schematic illustration of spunbond and melt-blown process (Edwards 2020, Hutten 2007)

The biggest difference between the spunbond and meltblown process involves the use of a die-assembly, as shown in **Figure 2** (Hutten 2007).

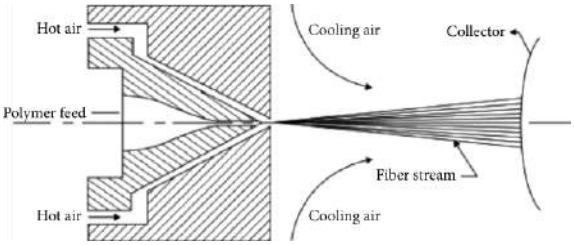


**Figure 2:** Schematic illustration of meltblown die-assembly (Hutten 2007)

The die-assembly, which is used in the production of melt-blown fibers, uses feed distribution to keep the raw polymeric materials flowing evenly throughout the manufacturing process (Hutten 2007). While an air manifold supplies hot high air velocity and a nosepiece ensures even filament diameter, an extruder with tiny nozzles pushes the filament, drawing the polymer into thin microfibers. As a result, the melt-blown fibers have very fine filament diameters, enabling the polypropylene to act as the main filtering agent in the COVID-19 face masks. By developing a strong understanding of the processes involved in making the plastic face mask filters, researchers can further investigate the fundamental properties of the filter's specific type of plastic.

In examining the properties of polypropylene, its favorable linear branched architecture can be observed. This type of architecture is indicative of its thermoplastic, or thermosoftening, behavior, where the slightly branched long chain molecules are able to be reheated, remolded, and cooled as necessary. This behavior explains polypropylene's widespread usage in products from insulated electrical cables to reusable plastic food containers. It is important to examine the specific type of polypropylene used, as the applications vary drastically with the polymeric

properties. Because of polypropylene's tacticity, there are three different types: isotactic, syndiotactic, and atactic, as shown in **Figure 3**.

**Figure 3:** Illustrations of the different orientations of polypropylene

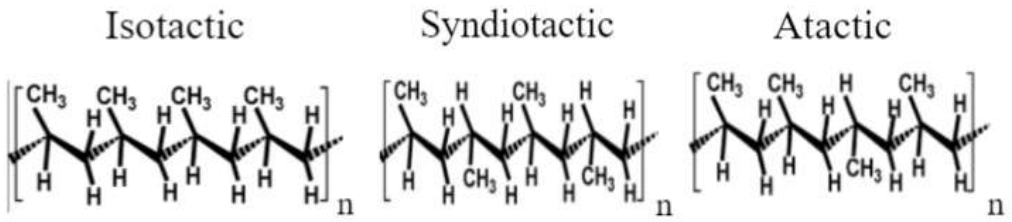


The changing position of the methyl group along the polypropylene backbone chain can drastically vary material properties and flexibility, as shown by **Table 1** (Hutten 2007, Rubenstein 2003). Isotactic polypropylene is the most commercially available and widely used of the three different types. It has methyl groups in the same position along the chain and monoclinic-alpha crystalline structure, giving the material a greater degree of crystallinity. As a result, the material is more stiff and resistant to creep. Syndiotactic polypropylene has methyl groups that alternate positions and orthorhombic crystalline structure, giving the material a lower degree of crystallinity. Atactic polypropylene has methyl groups in random positions with no crystal structure. In other words, atactic polypropylene is amorphous in structure, resulting in behaving similar to a gooey gel-like substance. Because of its favorable properties and use in COVID-19 face masks, isotactic polypropylene was chosen as the material to be researched within the scope of this project.

**Table 1:** Properties for isotactic, syndiotactic, and atactic polypropylene (Hutten 2007, Natta 1967, Rubenstein 2003)

| Property | Isotactic | Syndiotactic | Atactic |
|---|---|---|---|
| **Type of Structure** | Crystalline | Crystalline | Amorphous |
| **Structure Details** | Monoclinic (α-structure) | Orthorhombic | Not applicable |
| **Free Volume** | Lowest | Medium | Highest |
| **Melting Temperature** | 160 - 174 °C | 125 - 130 °C | Not applicable |
| **Glass Transition Temperature** | Not found | Not found | -17 - 0 °C |
| **Crystal Ratio** | 70 - 80% | ~50% | Not applicable |

The degree of crystallinity is another important parameter, as it explains whether a polymer melts like a typical solid or transitions between both glass and rubbery states. Highly crystalline materials, like isotactic polypropylene with a 70-80% crystal ratio and syndiotactic

polypropylene with a 50% crystal ratio, will have melting points, while highly amorphous materials, like atactic polypropylene will become rubbery over a certain range of temperatures (Hutten 2007). This insight explains why isotactic polypropylene and syndiotactic polypropylene show melting temperatures, while atactic polypropylene instead has a glass transition temperature.

Similarly, the transitions within the crystalline structure is yet another crucial parameter, as it uses free volume changes to explain how a polymer responds to different processes such as deformation, solid-phase reactions, and creep. By using a dynamic mechanical analysis (DMA) scan, it is possible to measure these different transitions in thermoplastics. As shown in **Figure 4**, these different transitions are labeled with greek letters including alpha, beta, and gamma (PerkinElmer 2007). These transitions are caused by molecular motions and free volume changes, and can define how a polymer will behave at a certain temperature.

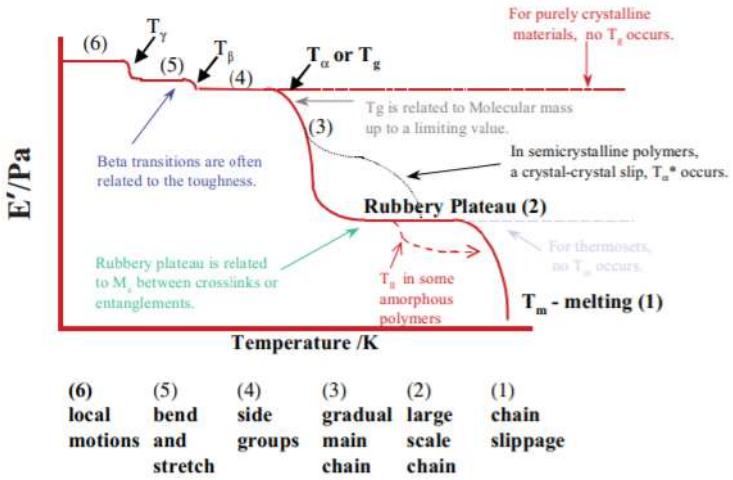


**Figure 4:** Idealized DMA scan showing the different types of transitions (PerkinElmer 2007).

The most important transition temperature is $T_a$, which is also known as the glass transition temperature $T_g$. $T_g$ is so critical because it marks the point at which major transitions occur for polymers, as physical properties change drastically from being hard and glassy to being soft and rubbery. This transition explains why poorly crystalline materials, such as atactic polypropylene, have glass transition temperatures and no melting temperatures, while highly crystalline materials, such as isotactic polypropylene and syndiotactic polypropylene, have no glass transition temperatures and do have melting temperatures. In the crankshaft model, it is possible to see how the polymers behave with the influence of temperature. As shown in **Figure 5**, molecules, or monomers, are seen as a series of jointed segments, or polymers (PerkinElmer 2007).

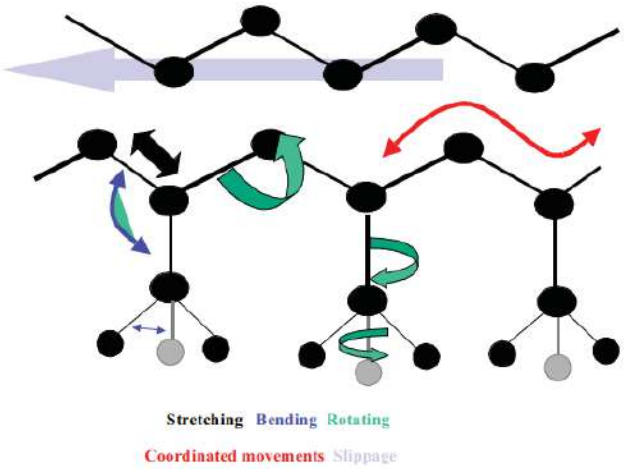


**Figure 4:** Schematic illustration of crankshaft model (PerkinElmer 2007)

At low temperatures when the chain is tightly pressed together, there is little mobility and therefore low free volume. At higher temperatures when the chain is not as tightly pressed together, there is increased mobility and therefore higher free volume. As the material increases in temperature, free volume increases and permits enhanced mobility for the side chains and small groups along the polypropylene backbone. As a result, there are different localized bond movements that are permitted, such as bending and stretching.

In examining polypropylene and its free volume, it is crucial to first consider Flory's Mean-Field Theory model. This model, which estimates energetic and entropic contributions to free energy, uses a lattice site model where sites can either be filled with monomers or solvents. However, one weak point of this model lies in the fact that free volume is ignored and accounted for via a "fudge factor." While this fudge factor value works for Mean-Field Theory applications, it cannot be ignored when handling polypropylene for research applications. According to Rubenstein and Colby, free volume is defined as the remaining fraction of a liquid's volume that is free for motion when molecules in a liquid occupy a majority of the liquid's volume (Rubenstein 2003). By applying this same definition to monomers and polymers, it is possible to understand the relationship between free volume and temperature, and free volume and mobility.

To further explore the relationship polypropylene has with temperature, it is important to examine a few different fundamental equations. The Williams, Landel, and Ferry equation (WLF) describes the temperature dependence of viscosity on polymer melts. As such, we can utilize the WLF equation to understand the time and temperature behavior of polymers in the glass transition region (**Eq. 1**).

$$\frac{\eta}{\eta_0} = \exp\left(B\left[\frac{1}{f} - \frac{1}{f_0}\right]\right)$$

$$\frac{\eta}{\eta_0} = \exp\left(\frac{B}{f_0}\frac{(T_0 - T)}{(T - T_\infty)}\right) \quad [1]$$

Where $\eta$ = Viscosity
$\eta_0$ = Viscosity at reference temperature
B = Empirical constant of order unity
$f$ = Fractional free volume
$f_0$ = Fractional free volume at reference temperature
T = Temperature
$T_0$ = Reference temperature
$T_\infty$ = Vogel temperature

## *Polypropylene in Additive Manufacturing*

Additive manufacturing, commonly called 3D printing, is a collective term for various manufacturing processes that form successive layers of material to form an end product. As mentioned in the introduction, this process has become the basis for an industry that has grown tremendously since its beginnings in the 1980s, with many applications taking advantage of its rapidity and flexibility of manufacture.

One of the most common methods of additive manufacturing, particularly for rapid prototyping and personal use, is that of extrusion-based systems wherein filaments of materials that melt and resolidify (such as thermoplastics like polypropylene) are wound up in spools. These filaments are then passed through a liquifier head to melt and then directed through extrusion nozzles to deposit a layer of material as the head moves in the X- and Y-directions. The head (or table) then move in the Z-direction to "print" the next layer. A simplified diagram of this process, known as *fused filament fabrication* (FFF), is shown in **Figure 5**.

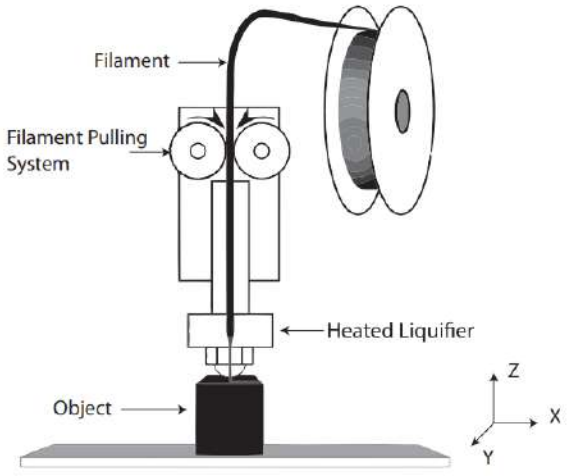


**Figure 5:** Diagram of a Fused Filament Fabrication Process (Carneiro et al. 2015)

As the filaments are deposited in the layers, their cylindrical shape means that it is not possible to completely fill the volume of the printed object. Due to this noncontinuous nature, parts made through FFF are weaker mechanically than parts made through more traditional manufacturing techniques, and must be made of higher performance materials. Thus, common materials used in FFF include high-performance polymers such as polylactic acid (PLA), acrylonitrile butadiene styrene (ABS), nylon, and polycarbonate (Roberson 2021).

Isotactic polypropylene, as a semi-crystalline polymer, should be included; however, that very semi-crystalline nature introduces its own problems. As the polypropylene chains order themselves into crystals, the volume occupied by the chains decreases compared to the amorphous structure prevalent in the melt. This in turn causes the finished printed part to experience shrinkage and warpage of its structure as it cools, both within the printed and from a poor adhesion of polypropylene to the printing bed. The cooling rate greatly affects this decrease in volume, as a lower cooling rate leads to a higher degree of crystallinity and subsequently a greater shrinkage. To demonstrate this volume change due to temperature, a comparison of the coefficient of linear thermal expansion (CTE) for polypropylene, as well as several of the aforementioned polymers used in FFF, is shown below in **Table 2** (data from SpecialChem SA). An example of a structure printed out of isotactic polypropylene showing the shrinkage typical of this material is shown in **Figure 6**; the post-print dimensional deviation is most evident at the corners of what is supposed to be a box.

**Table 2:** Linear Coefficients of Thermal Expansion for Different Polymers and Cellulose

| **Material** | **Linear Coefficient of Thermal Expansion ($10^{-5}$/°C)** |
|---|---|
| ABS | 7-15 |
| PLA | 8.5 |
| Isotactic PP | 7-17 |
| Cellulose Fiber | 1-18 |

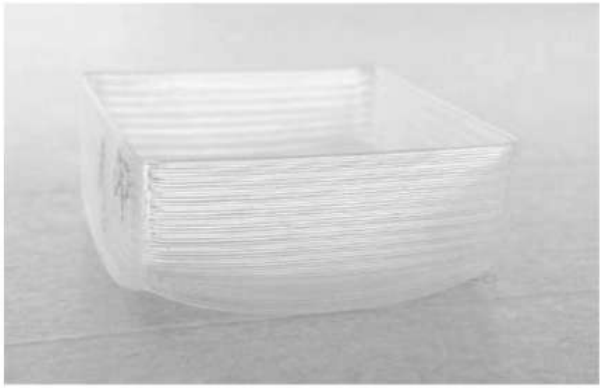

**Figure 6:** FFF manufactured structure showing shrinkage after printing (Carneiro et al. 2015)

As can be seen in **Table 2**, the materials mostly have a range of values for the CTE. This is due to the dependence of the coefficient to intermolecular forces: the more internal bonds between molecules, the more a given material will expand. Thus the coefficient of linear thermal expansion depends on molecular weight (a proxy measurement for chain length), where a longer chain would have lower coefficient as there would be fewer internal bonds per unit volume than a chain with lower molecular weight (Chemical Retrieval on the Web).

To address the higher shrinkage experienced by isotactic polypropylene, this paper proposes the incorporation of an additive to the polymer matrix, specifically cellulose, to modify the physical properties of the composite and achieve a material with higher dimensional stability. Cellulose can have this effect on polypropylene for two reasons: first, **Table 2** shows that cellulose has a smaller CTE, and therefore a composite of cellulose and polypropylene would have a CTE in between that of the pure materials, importantly lower than that of polypropylene; secondly, cellulose can inhibit the crystallization of polypropylene by displacing the polymer and interfering with diffusion and chain folding, and with a lower crystallization ratio there would be less shrinkage after printing.

# Research Plan

### *Recovery of Polypropylene*

As stated earlier, the first goal is to recover polypropylene from disposable masks used during the COVID-19 pandemic. In order to achieve this goal, we will utilize a technique called the Solvent-targeted Recovery and Precipitation (STRAP) method. This method was chosen because it can be used to selectively extract polymers from one another at a high efficiency. The method uses a solvent to selectively dissolve one polymer of a mixture. The solvent used is generally one in which the desired polymer, in our case polypropylene, is highly soluble and the other polymers are insoluble. Once the desired polymer is dissolved, it is filtered and recovered by precipitation in a poor solvent and then filtered again to ensure purity. This technique is also useful if multiple polymers require extraction by using additional solvents for dissolving and precipitating those polymers (Walker, 2020).

Several key fundamentals of polymer physics need to be taken into account when choosing good solvents for dissolving the desired polymer and poor solvents for precipitating the polymer. The first is an understanding of the thermodynamics of mixing. The mixing of a polymer and solvent are governed by the Gibbs or Helmholtz free energy of the system. In order for mixing to be favorable and a solvent to be considered a good solvent, the free energy must be minimized which will ensure that the polymer and solvent are miscible. Generally, polymers will be soluble in solvents with similar properties to themselves (Rubinstein, 2003). For polypropylene, this would mean that a nonpolar solvent would be required for the dissolutions part of the procedure. For example, xylene is a nonpolar solvent which has been shown to effectively dissolve polypropylene (Poulakis & Papaspyrides, 1997). A poor solvent is required for the precipitation of polymers. This entails a positive free energy, making the polymer and solvent immiscible. In this case, the polymer molecules prefer to interact with one another rather than with the solvent molecules and will precipitate out of solution. This generally requires the use of a solvent with different properties than the polymer (Rubinstein, 2003). Acetone is a known poor solvent of polypropylene due to its polar nature, and has been used to precipitate polypropylene out of solution (Poulakis & Papaspyrides, 1997).

The free energy of mixing is directly influenced by the entropy and enthalpy of the system. For mixing to occur, the entropy should be maximized while the enthalpy should be minimized. The entropy of mixing is generally positive and favorable. The general definition of entropy is related to the number of ways molecules can be arranged in a system (**Eq. 2**). When sets of different molecules are mixed together, the number of possible arrangements increases which increases the entropy (Rubinstein, 2003).

$$S = k \ln \Omega \quad [2]$$

Where S = Entropy
k = Boltzmann's constant
Ω = Degrees of freedom

Flory's mean field theory can be used to calculate the entropy upon mixing by modeling the polymer-solvent system as a lattice upon which each molecule occupies a lattice site. As such, we can utilize the volume fractions of the polymer and solvent and the number of occupied lattice sites to determine the entropy of mixing (**Eq. 3**)(Rubinstein, 2003).

$$\Delta \bar{S}_{mix} = -k \left[ \frac{\phi_{PP}}{N_{PP}} \ln \phi_{PP} + \phi_{Solvent} \ln \phi_{Solvent} \right] \quad [3]$$

Where $\phi_{PP}$ = volume fraction of polypropylene
$\phi_{solvent}$ = volume fraction of solvent
$N_{PP}$ = number of lattice sites occupied by polypropylene

The enthalpy of mixing is governed by the interaction energies of the polymer with itself, the polymer with the solvent, and the solvent with itself. Since the entropy always promotes mixing, solubility of a polymer in a solvent is largely dependent on these interaction energies. The interaction energies are included in the Flory interaction parameter, χ (**Eq. 4**)(Rubinstein, 2003).

$$\chi \equiv \frac{z}{2} \frac{\left( 2u_{PP\_Solvent} - 2u_{PP\_PP} - u_{solvent\_solvent} \right)}{kT} \quad [4]$$

Where $u_{PP\_Solvent}$ = interaction energy between polypropylene and the solvent
$u_{PP\_PP}$ = interaction energy between polypropylene and itself
$u_{solvent\_solvent}$ = interaction energy between the solvent and itself
T = temperature
z = number of surrounding lattice sites

The Flory interaction parameter can be used to calculate the enthalpy of mixing (**Eq. 5**) (Rubinstein, 2003).

$$\Delta \bar{U}_{mix} = \chi \phi (1 - \phi) kT \quad [5]$$

Where $\phi$ = volume fraction of polypropylene

The total free energy of the system is calculated by combining the entropy and enthalpy of mixing (**Eq. 6**). Since Flory's mean field theory operates under the assumption that there is no change in volume upon mixing, the Helmholtz free energy is used(Rubinstein, 2003).

$$\Delta \bar{F}_{mix} = kT \left[ \frac{\phi}{N} \ln \phi + (1 - \phi) \ln(1 - \phi) + \chi \phi (1 - \phi) \right] \quad [6]$$

In order to minimize the free energy to promote mixing of the polymer with the solvent, making them miscible and the solvent a good solvent, Flory's interaction parameter, χ, must be negative which is necessary for the first step of dissolving the polypropylene using the STRAP method. If χ is positive, the polymer will be insoluble in the solvent, making it a poor solvent, and the

polymer would precipitate out of the mixture, which is necessary for the third step of the STRAP method (Rubinstein, 2003).

In order to gauge solubility of a polymer within a solvent, the solubility of the polymer and of the solvent can be compared. The Hildebrand-Scott solubility parameter (**Eq. 7**), describes the interaction energy of the molecules as the square-root of the cohesive energy density. The cohesive energy density describes the interaction energy per unit volume of the molecules in their pure state. The interaction energy is expressed as the energy of vaporization which is the amount of energy required to separate one molecule from all of its neighboring molecules to remove it from solution (Rubinstein, 2003).

$$\delta \equiv \sqrt{\frac{\Delta E_{PP}}{v_{PP}}} \qquad [7]$$

Where $\delta$ = solubility parameter
$\Delta E_{PP}$ = energy of vaporization of polypropylene
$v_{PP}$ = volume of polypropylene

This form of the solubility parameter is generally acceptable for nonpolar molecules like polypropylene. However, other solubility parameters need to be taken into account for molecules that exhibit polarity or hydrogen bonding. Charles Hansen developed solubility parameters to account for the main types of interactions exhibited by different types of molecules including one for dispersion forces, $\delta_D$ , one relating to dipole moment and polarity, $\delta_P$, and one for hydrogen bonding, $\delta_H$. These solubility parameters can be used to measure the difference, Ra, between two types of molecules such as a polymer and a solvent (**Eq. 8**). A smaller difference, Ra, between a polymer and a solvent indicates a stronger likelihood of the polymer being dissolved in that solvent (Hansen, 2007).

$$Ra^2 = 4(\delta D_1 - \delta D_2)^2 - (\delta P_1 - \delta P_2)^2 - (\delta H_1 - \delta H_2)^2 \qquad [8]$$

Since polypropylene is a nonpolar molecule, the only applicable Hansen solubility parameter is the one for dispersion forces as can be seen from their values which are $\delta D = 18.0\ MPa^{1/2}$, $\delta P = 0\ MPa^{1/2}$, and $\delta H = 0\ MPa^{1/2}$ (Barton, 1991). The values for $\delta P$ and $\delta H$ are both zero since polypropylene does not exhibit any hydrogen bonding and is not polar (Hansen, 2007).

A simple method can be used to estimate the solubility parameter of polypropylene based on the group contributions of functional groups (**Eq. 9**) (Painter & Coleman, 2008).

$$\delta = \frac{\sum_i F_i^*}{\sum_i V_i^*} \qquad [9]$$

Where $F_i^*$ = molar attraction constant for *i*th group
$V_i^*$ = molar volume constant for *i*th group

Using the constant values in **Table 3**, the value of the solubility parameter for polypropylene was determined to be 7.43 $(cal.cm^{-3})^{0.5}$(Painter & Coleman, 2008).

**Table 3**: Values for the molar attraction and molar volume constants for functional groups in PP.

| Group | Molar Attraction Constant ($F^*$, $(cal.cm^3)^{0.5}mole^{-1}$) | Molar Volume Constant ($V^*$, $cm^3\ mole^{-1}$) |
|---|---|---|
| $CH_3$ | 218 | 31.8 |
| $-CH_2-$ | 132 | 16.5 |
| >CH- | 23 | 1.9 |

## Experimental Procedure

In order to extract the PP from the masks, we will first determine appropriate good and poor solvents for PP using the polymer physics fundamentals mentioned above. The PP layer will be mechanically separated from the other mask layers. We will then dissolve the PP layer in xylene or another predetermined good solvent at a suitably high temperature after which the solution will be mechanically filtered. The PP will then be precipitated using acetone or another poor solvent and by decreasing the temperature. The precipitated product will then be dried and used for additive manufacturing.

### *Cellulose and Polypropylene: A Composite*

*Aim 2*: Synthesize a more sustainable, extrudable polymer filament for additive manufacturing using the recovered PP from disposable Covid-19 face masks.

PP is not widely used in additive manufacturing due to the issues mentioned above, however, it is possible to modify the PP matrix with fillers or additives to alter its physical properties during and after the printing process. Additionally, additive manufacturing has recently seen a trend toward sustainability with the use of abundant biomass materials as modifying agents[X]. Therefore, in an effort toward increasing sustainability, our group proposes to modify PP with cellulose, a natural polymer found in plants and agricultural byproducts. The main objectives that this section explores are (i) can we create a stable, miscible PP-cellulose polymer blend, (ii) if so, can the PP-cellulose polymer blend be utilized as an extrudable filament for FDM additive manufacturing, and (iii) what work has already been done in this regard and can we improve upon it in an effort to decrease its environmental impact?

Cellulose is a complex carbohydrate (i.e., polysaccharide) found in the cell wall of nearly all plant matter. More specifically, cellulose is a linear chain of glucose molecules ($(C_6H_{10}O_5)n$; n=10,000 to 15,000) linked together through acetal oxygen, covalently bonding C1 of one glucose ring and C4 of the adjoining ring (USFS Forest Products Laboratory, Purdue University). Cellulose chains are hydrogen bonded together, forming elementary fibrils which contain disordered (amorphous) and highly ordered (crystalline) regions. The cellulose monomer, shown in **Figure 7** (Painter & Coleman, 2009), is polar and hydrophilic due to the alcohol groups attached to the carbon rings and therefore makes cellulose (or any plant based materials) susceptible to moisture. Cellulose fibrils are the main reinforcement in plant cell walls, giving

plants their sturdy structure. Wood has a hierarchical and cellular structure composed mainly of cellulose, lignin, and hemicellulose (the chemical building blocks) where cellulose microfibrils are organized in defined oriented layers embedded in a hemicellulose and lignin matrix (**Figure. 8**) (Gauss *et al*. 2020). Softwoods and hardwoods contain the most cellulose content (~48 wt.%). Non-wood biomasses, e.g. banana waste, sugar cane bagasse, corn cobs, and sponge gourd fibers, contain anywhere from ~13 wt.% to ~67 wt.%, as seen in **Table 4** (Shahzadi *et al.* 2014).

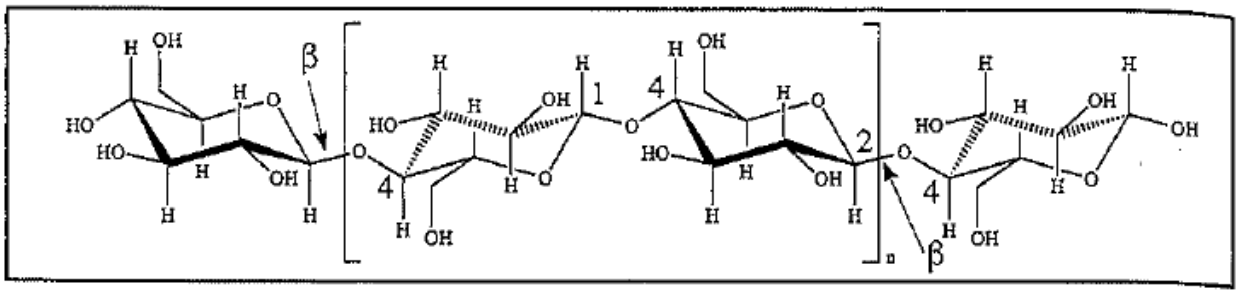

**Figure 7**: The chemical structure of cellulose. The cellulose monomer is depicted in brackets.

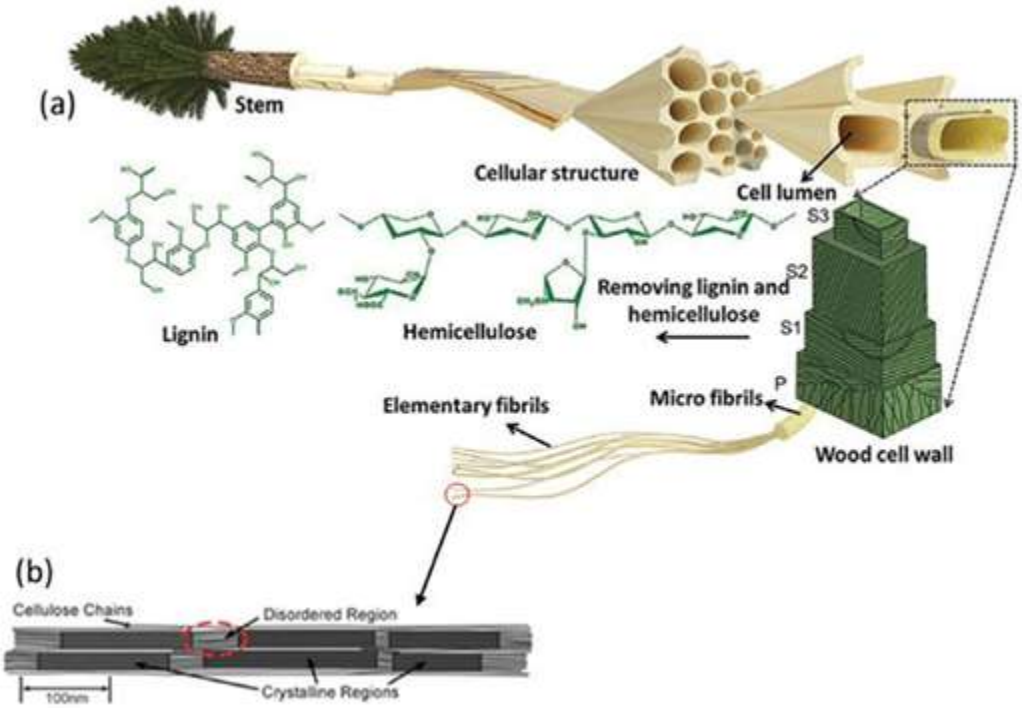


**Figure 8**: (a) The hierarchical structure of a tree showing the cellulose organization within wood. (b) Cellulose microfibrils contain elementary fibrils with crystalline (containing cellulose nanocrystals) and amorphous (disordered) regions.

| Lignocellulosic material | Lignin (%) | Hemicellulose (%) | Cellulose (%) | Reference* |
|---|---|---|---|---|
| Sugar cane bagasse | 20 | 25 | 42 | Kim & Day, 2011 |
| Sweet sorghum | 21 | 27 | 45 | Kim & Day, 2011 |
| Hardwood | 18 - 25 | 24 - 40 | 40 - 55 | Malherbe & Cloete, 2002 |
| Softwood | 25 - 35 | 25 - 35 | 45 - 50 | Malherbe & Cloete, 2002 |
| Corn cobs | 15 | 35 | 45 | Prassad *et al.* 2007 |
| Corn stover | 19 | 26 | 38 | Zhu *et al.* 2005 |
| Rice Straw | 18 | 24 | 32.1 | Prassad *et al.* 2007 |
| Nut shells | 30 - 40 | 25 - 30 | 25 - 30 | Abbasi & Abbasi, 2010 |
| Newspaper | 18 - 30 | 25 - 40 | 40 - 55 | Howard *et al.* 2003 |
| Grasses | 10 - 30 | 25 - 50 | 25 - 40 | Malherbe & Cloete, 2002 |
| Wheat straw | 16 - 21 | 26 - 32 | 29 - 35 | McKendry, 2002 |
| Banana waste | 14 | 14.8 | 13.2 | John *et al.* 2006 |
| Bagasse | 23.33 | 16.52 | 54.87 | Guimarães *et al.* 2009 |
| Sponge gourd fibers | 15.46 | 17.44 | 66.59 | Guimarães *et al.* 2009 |

**Table 4**: Percent composition of lignocellulose components in common biomass materials.

Several commercial processes in the paper industry including the kraft method (using sodium hydroxide or sodium sulfide) and the organosolv method (using ethanol and water) are used to extract all constituents in the biomass material, leaving cellulose behind. In both methods, elevated temperature and pressure are required to remove the lignin and hemicellulose.

Cellulose nanofibrils are classified according to their structure and morphology e.g., cellulose microfibre (MF), microcrystalline cellulose (MCC), cellulose nanocrystal (CNC), nanofibrillated cellulose (NFC), bacterial cellulose particles (BC), regenerated cellulose (RC), etc. The main difference between these cellulose types is blank… nano- vs. microcellulose. Each cellulose-compound can vary in size, shape, and properties enabling different uses of cellulose for different purposes in 3D printing i.e., as a rheology modifier, binder, excipient, matrix, and/or a reinforcement, as shown in **Table 5** (Gauss *et al*. 2020).

| Use of cellulose | Properties that enable the use of cellulose | Application in 3D printing |
|---|---|---|
| Rheology modifier | Neighbouring chains in cellulose form hydrogen bonds, restricting the water motion and increasing the viscosity. At a high shear rate, hydrogen bonds break through shear thinning behaviour. | Cellulose has suitable rheological properties for 3D inks as the ink flows smoothly at high shear rates and quickly solidifies once the printing stops. |
| Binder | Cellulose has shear thinning behaviour making it a good choice of binder for 3D printing powders | Rheology of a 3D printing paste depends on the rheology of a binder. Shear-thinning property of the cellulose binder helps in achieving a successful print. |
| Excipient | Hydrophilic nature of cellulose helps achieve controlled swelling on contact with water. | This property of cellulose can be exploited in applications such as drug delivery and 4D printing |
| Matrix | High molecular weight cellulose dissolved by solvents has a high viscosity and exhibits shear thinning. | High viscosity solubilised cellulose is suitable for 3D printing methods such as material extrusion method to produce dimensionally stable prints |
| Reinforcement | Cellulose fibres exhibit high strength, high stiffness, and low density | Cellulose fibres extruded with thermoplastics are commonly used as filaments or used in bioink formulations. 3D printed cellulose-based composites have shown improved mechanical properties |

**Table 5**: Uses of celluose in 3D printing.

Due to the fact that we propose to mix isotactic PP and cellulose, we expect certain issues upon mixing i.e., isotactic PP is nonpolar *and* hydrophobic (due to the methyl groups), while cellulose

is polar *and* hydrophilic (due to the alcohol groups). Thus, mixing will have a two fold issue of incompatibile (1) hydrophobicity and (2) polarity. As introduced in Aim 1, Flory's mean field theory is used to estimate the entropy upon mixing of the cellulose and PP, polymer-polymer system, such that,

$$\Delta\bar{S}_{mix} = -k\left[\frac{\varphi_{PP}}{N_{PP}}\ln(\varphi_{PP}) + \frac{\varphi_{cellulose}}{N_{cellulose}}\ln(\varphi_{cellulose})\right]$$

Where $\phi_{PP}$ = volume fraction of polypropylene
$\phi_{Cellulose}$ = volume fraction of solvent
$N_{PP}$ = number of lattice sites occupied by polypropylene
$N_{Cellulose}$ = number of lattice sites occupied by polypropylene

Entropy always promotes mixing (a large negative number), however, due to the compatibility issues mentioned above, it is expected that the entropy of mixing PP and cellulose will be a small negative number. Polymer blends with small entropy of mixing values typically phase separate or are immiscible.

There are several known ways to improve the compatibility of PP and cellulose. A chemical surface treatment of mercerization, followed by esterification, has been shown to expose the hydroxyl (-OH) groups on the cellulose surface and then transform them into ester bonds to increase the hydrophobicity of cellulose. Afterwhich, cellulose can be covalently grafted to maleated PP (MAPP) to create a miscible polymer-polymer blend. We will continue to use the Flory-Huggins Mean-Field Theory and related equations to further explore the polymer physics behind each step.

## Chemical Surface Treatment

Step (a): mercerization is the process of treating a material, or polymer in our case, with a caustic solution to alter the fibers in the molecules and ultimately change the properties of the material (Zhang *et al.,* 2017). Here, cellulose is mixed with an aqueous NaOH solution (i.e., Na+ and OH- ions) to expose -OH reactive sites. The NaOH solution acts as a good solvent when mixed with cellulose, thus causing the cellulose polymer to swell, exposing more and more reactive hydroxyl groups on the cellulose chains. The OH sites react with the OH- anions to create water and deprotonate the hydroxyl groups on the cellulose chains into alkoxides (**Figure 9**). The alkoxides are then protonated back into OH sites via a water wash and the alkaline chemical treatment is repeated. Each time this is repeated, the cellulose crystalline regions become more amorphous as its surface is swollen, exposed, and modified. The purpose of this step is to increase the number of reactive sites and amorphousness for step (b) and clean the cellulose of any impurities (e..g., wax, oil, debris, etc.).

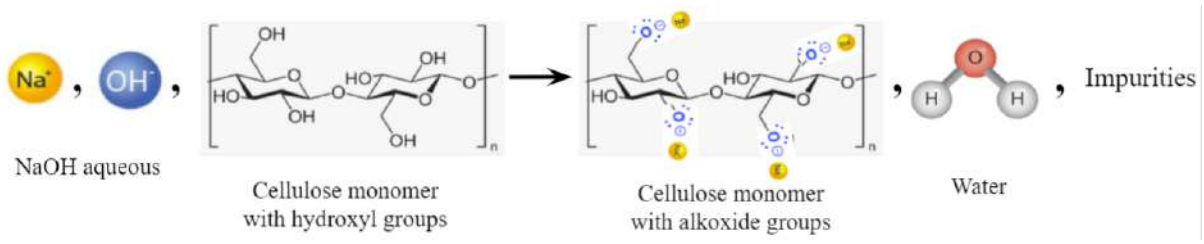

**Figure 9**: Alkaline chemical surface treatment to increase the number of reactive hydroxyl groups on cellulose and decrease the crystalline regions.

Step (b): esterification is the process of combining an organic acid with an alcohol to form at least one ester product and water (Zhang *et al.,* 2017). Here, cellulose is mixed with acetic acid, which acts as a good solvent to swell the cellulose polymer. Afterwhich, the cellulose is reacted with acetic anhydride at a high temperature. The acetylating agents react with the numerous exposed, hydrophilic hydroxyl groups and convert them into esters, which are more hydrophobic. Increasing the hydrophobicity of the cellulose chains improves its compatibility with PP which is a hydrophobic polymer. Note that diffusion is difficult in high crystalline regions, thus, increasing the amorphousness of cellulose in step (a) is critical for the effectiveness of step (b).

The Flory interaction parameter, introduced in Aim 1, can also be written as

$$\chi = z\Delta\varepsilon\_(Cellulose - PP)/kT$$

Where z = number of surrounding lattice sites or neighbors
$\Delta\varepsilon_{Cellulose\text{-}PP}$ = energy change per cellulose-PP interaction pair
K = Boltzmann's constant
T = temperature

The interaction parameter and temperature have an inverse relationship, thus, increasing the temperature during step (b) decreases the interaction parameter between cellulose and PP interaction pairs. Decreasing the interaction parameter, decreases the strength of the enthalpy term in the change in free energy due to mixing (Flory-Huggins equation),

$$(\Delta G\_mix)/RT = [\![n\_A\ ln]\!](\varphi\_A) + [\![n\_B\ ln]\!](\varphi\_B) + n\_A\ \varphi\_B\ \chi$$

Where $\phi_{Cellulose}$ = volume fraction of cellulose
$\phi_{PP}$ = volume fraction of polypropylene
$n_{Cellulose}$ = number of lattice sites occupied by cellulose
$n_{PP}$ = number of lattice sites occupied by polypropylene
R = molar gas constant
T = temperature
$\chi$ =interaction parameter

The first two terms are entropic while the last term in Eq. X is enthalpic. Decreasing the (positive) enthalpy term means the two (negative) entropy terms dominate the equation and the free energy of mixing becomes more negative and thus more favorable.

## Covalent Grafting

Maleic anhydride is now covalently grafted onto the backbone of PP to create maleated polypropylene. The MA groups on PP can then be reacted with the OH groups on cellulose via covalent bonds to yield a cellulose-MAPP polymer blend (**Figure 10**). It has been reported that the surface energy of cellulose decreases once reacted with the MA groups on PP, improving the interfacial adhesion between the natural polymer and PP matrix (Zhang *et al.,* 2017).

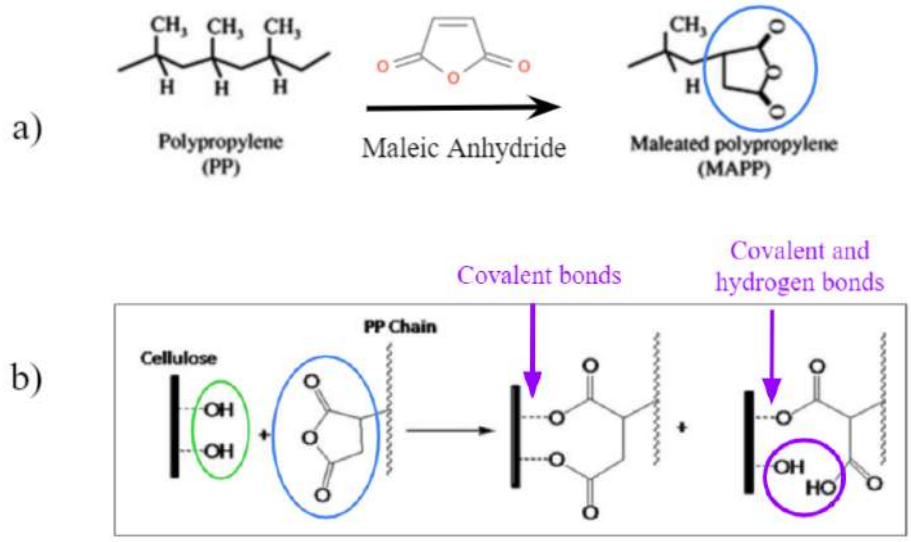


**Figure 10.** Covalent grafting of Cellulose and Maleated Polypropylene. (a) Polypropylene is maleated by maleic anhydride. (b) Reactive hydroxyl groups on cellulose react with maleic anhydride groups on maleated polypropylene via covalent and/or hydrogen bonds.

To further understand this claim, we consider how surface energy affects the free energy of mixing. Surface energy of a molecule is also known as its energy of vaporization (i.e., how much energy is needed to completely separate the molecules away from each other). As introduced for Eq. 7, surface energy, cohesive energy density, and the Hildebrand-Scott solubility parameter are related. Equation 7 can also be written as

$$\delta\_A = \sqrt{\Delta EAA/vAA} = C\_AA\text{^}0.5$$

Where $\delta_A$ = solubility parameter of polymer A

$\Delta E_{AA}$ = energy of vaporization of interaction pair AA

$v_{AA}$ = volume of interaction pair AA

$C_{AA}$ = cohesive energy density of interaction pair AA

The cohesive energy density (CED) and solubility parameter are alternative ways to describe interactions in polymer science and thus are related. Solubility parameter can be determined from pure component properties, while $\chi$ was designed to be an adjustable parameter that would be determined by a fit to experimental data.

The change in solubility parameter between polymers influences the change in enthalpy of mixing (also referred to as the heat of mixing) of the polymer blend and can be written as

$$\Delta H\_mix = (n\_A + n\_B)\, V\_mix\, \Phi\_A\, \Phi\_B\, (\delta\_A - \delta\_B)\text{^}2$$

Where $n_A$ = number of lattice sites occupied by polymer A

$n_B$ = number of lattice sites occupied by polymer B

$V_{mix}$ = volumar volume of the mixture

$\phi_A$ = volume fraction of polymer A

$\phi_B$ = volume fraction of polymer B

$\delta\_A - \delta\_B$= change in solubility parameter of polymer blend AB

As the solubility parameter of polymer A and polymer B become closer in value, the change in solubility parameter of the polymer blend AB becomes smaller, decreasing the overall enthalpic contribution. This is important when considering the Flory-Huggins free energy of mixing relationship,

$$\Delta Gmix = \Delta H\_mix - T\Delta S\_mix$$

Where $\Delta H_{mix}$ = enthalpy (or heat) of mixing
$\Delta S_{mix}$ = entropy of mixing
T = temperature

Therefore, as the change in solubility parameter of the polymer blend AB becomes smaller, enthalpy of mixing decreases, and entropy of mixing becomes the dominant term in the free energy of mixing equation. The entropic term is always negative, thus, the free energy of mixing polymer blend AB becomes more negative and is a more energetically favorable mixture. Favorable mixtures are miscible and are not likely to phase separate.

In order to see the change in solubility parameter of our final cellulose-PP mixture, we first calculate the initial solubility parameter of all five possible starting materials: (1) polypropylene, (2) maleated polypropylene, (3) cellulose, (4), maleated cellulose, and (5) cellulose-maleated polypropylene blend. Each monomer is depicted in **Figure 11**, respectively. The solubility parameter of each material is calculated according to Eq. 9 using the Group Contribution Method (Painter & Coleman, 2009). Additionally, the cellulose-MAPP blend has three possible configurations depending on how the MA group from MAPP bonds to one of the three available OH groups from cellulose, shown in **Figure 12** (Uetsuji *et al.*, 2020). All calculations are shown below.

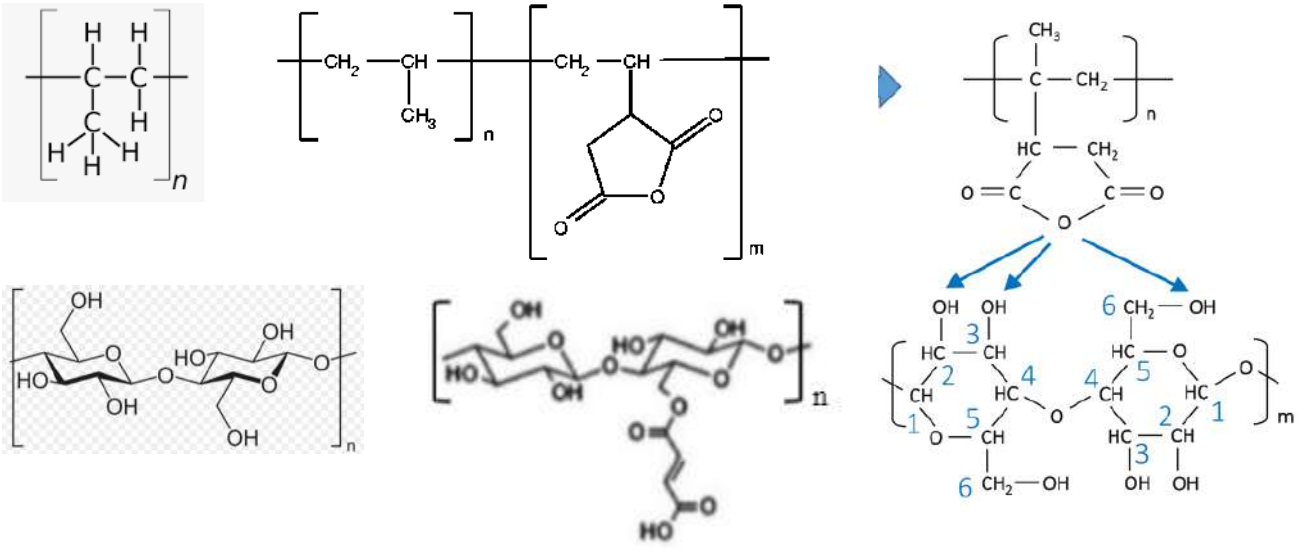

**Figure 11**: The polymer or polymer blend monomers of (a) polypropylene, (b) maleated polypropylene, (c) cellulose, (d) maleated cellulose, and (e) cellulose - maleated polypropylene.

$$\delta_{PP} = \frac{218 + 132 + 23}{31.8 + 16.5 + 1.9} = 7.43 \left(\frac{cal.}{cm^3}\right)^{0.5}$$

$$\delta_{MAPP} = \frac{218 + 3(132) + 3(23) + 95 + 2(18)}{31.8 + 3(16.5) + 3(1.9) + 5.1 + 2(-2.4)} = 9.32 \left(\frac{cal.}{cm^3}\right)^{0.5}$$

$$\delta_{Cellulose} = \frac{2(132) + 10(23) + 4(95)}{2(16.5) + 10(1.9) + 4(5.1)} = 12.07 \left(\frac{cal.}{cm^3}\right)^{0.5}$$

$$\delta_{MA-Cellulose} = \frac{2(132) + 10(23) + 5(95) + 2(18) + 2(113)}{2(16.5) + 10(1.9) + 5(5.1) - 2(2.4) + 2(13.7)} = 12.30 \left(\frac{cal.}{cm^3}\right)^{0.5}$$

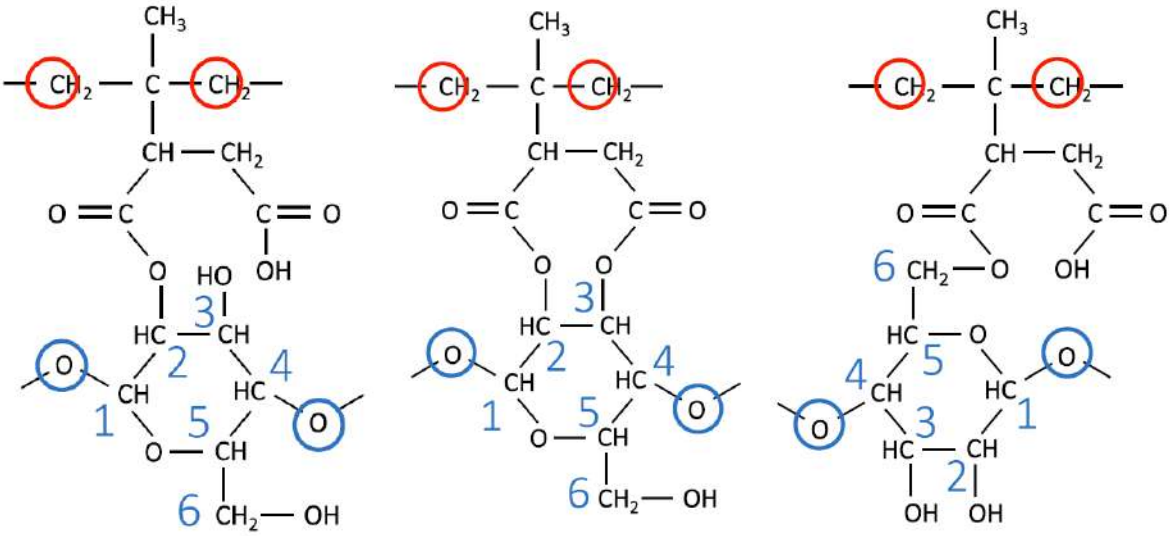

**Figure 12**: Three different possible configurations of Cellulose-Maleated Polypropylene (Cellulose-MAPP) polymer blend: (a) C2 model with monoester bond, (b) C2&C3 model with diester bond, and (c) C6 model with monoester bond.

$$\delta_{C2\ Model} = \frac{218 + 4(132) + 6(23) - 97 + 18 + 3(95) + 298}{31.8 + 4(16.5) + 6(1.9) - 14.8 - 2.4 + 3(5.1) + 19.6} = 10.94 \left(\frac{cal.}{cm^3}\right)^{0.5}$$

$$\delta_{C2\&C3\ Model} = \frac{218 + 4(132) + 6(23) - 97 + 3(95) + 2(298)}{31.8 + 4(16.5) + 6(1.9) - 14.8 + 3(5.1) + 2(19.6)} = 11.20 \left(\frac{cal.}{cm^3}\right)^{0.5}$$

$$\delta_{C6\ Model} = \frac{218 + 4(132) + 6(23) - 97 + 18 + 4(95) + 298}{31.8 + 4(16.5) + 6(1.9) - 14.8 - 2.4 + 4(5.1) + 19.6} = 11.23 \left(\frac{cal.}{cm^3}\right)^{0.5}$$

The individual and averaged solubility parameter and cohesive energy density values are shown in **Table 6** below. Regardless of how cellulose bonds to MAPP, the solubility parameters for all three configurations are relatively close in value and average to 11.12 $(cal./cm^3)^{0.5}$. Comparing the surface energy of pure cellulose (proportional to CED = $(12.07)^2 = 145.68$ $cal./cm^3$ from above) and the surface energy of cellulose-MAPP (CED = $(11.12)^2 = 123.65$ $cal./cm^3$), we can conclude that the surface energy of pure cellulose does indeed decrease when cellulose is reacted with the MA group on MAPP.

**Table 6**: Cohesive energy density(proportional to surface energy) comparison of all three possible configurations of the Cellulose-MAPP polymer blend.

| Cellulose-MAPP Blend | Solubility Parameter $(Cal/cm^3)^{1/2}$ | CED $(Cal/cm^3)$ |
|---|---|---|
| C2 Model | 10.94 | 119.68 |
| C2&C3 Model | 11.20 | 125.44 |
| C6 Model | 11.23 | 126.11 |
| **Average** | **11.12** | **123.65** |

The change in solubility parameter for each cellulose-PP blend combination is shown in **Table 7** below. The MA-Cellulose + PP polymer blend has the largest change in solubility parameter upon mixing (4.87 $(cal./cm^3)^{0.5}$) and is therefore, the least energetically favorable polymer blend and the most likely to phase separate. Conversely, the Cellulose + MAPP polymer blend has the smallest change in solubility parameter upon mixing (2.75 $(cal./cm^3)^{0.5}$) and is therefore, the most energetically favorable polymer blend and the least likely to phase separate. Thus, the Cellulose + MAPP polymer blend has the lowest free energy of mixing, is the most stable combination, and the best choice to use as an extrudable filament for additive manufacturing.

**Table 7**: Change in solubility parameter (proportional to change in free energy due to mixing) of all four possible combinations of Cellulose-Polypropylene polymer blends.

| Polymer Blend | Change in Solubility Parameter $(Cal/cm^3)^{1/2}$ |
|---|---|
| Δδ_(MACellulose-PP) | 4.87 |
| Δδ_(Cellulose-PP) | 4.64 |
| Δδ_(MACellulose-MAPP) | 2.98 |
| Δδ_(Cellulose-MAPP) | 2.75 |

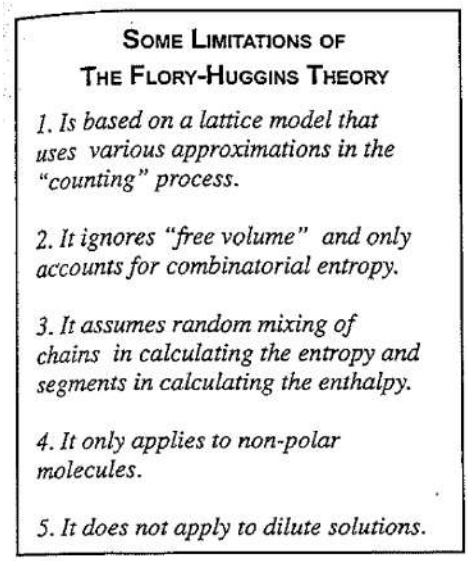


**Figure 12**: Limitations of the Flory-Huggins Theory (Painter & Coleman, 2009).

It is important to note that the Flory-Huggins Theory has several limitations (as listed in **Figure 12**). Limitation 4. "It only applies to non-polar molecules" is applicable to our situation as cellulose is a polar molecule. However, we believe this theory still gives good estimations for all calculated change in solubility parameter values in Table X, as the solubility parameter for cellulose is included in all four values. If there are any errors in the cellulose solubility parameter, it is included evenly in all four values, not in one value in particular, and still gives reasonable comparison values.

# Conclusion

One negative aspect of the COVID-19 global pandemic has been the vast increase in single-use plastic items entering the waste stream. The filter layer of these masks is made primarily of isotactic polypropylene, a high-performance polymer due to its chemical and structural makeup. This paper proposes a method to recover polypropylene from the single-use masks and modify its structure to allow it to be mixed with cellulose-based additives. Solvent-targeted recovery and precipitation (STRAP) methods would allow the extraction of polypropylene with minimal

contamination from the facemasks, while also serving a sterilizing effect. Structural modification of the polypropylene chains by grafting maleic acid and chemical treatment of cellulose would allow for these materials dissimilar in polarity to mix without experiencing phase separation. ONce so modified, the cellulose-polypropylene composite could be used in additive manufacturing, thus providing a new high-performance material for a growing industry while simultaneously helping to address a modern pollution problem.

# References


Akber Abbasi, Saddam, et al. “Extensive Use of Face Masks during COVID-19 Pandemic: (Micro-)Plastic Pollution and Potential Health Concerns in the Arabian Peninsula.” *Saudi Journal of Biological Sciences*, vol. 27, no. 12, 2020, pp. 3181–86. *Crossref*, doi:10.1016/j.sjbs.2020.09.054.

AMFG. “The Additive Manufacturing Industry Landscape 2020: 240 Companies Driving Digital Manufacturing [Updated].” *AMFG*, 18 Dec. 2020, amfg.ai/2020/05/26/the-additive-manufacturing-industry-landscape-2020-231-companies-driving-digital-manufacturing.

Barton, Allan F.M. “CRC Handbook of Solubility Parameters and Other Cohesion Parameters.” 2nd ed. (1991)

Carneiro, O. S., et al. “Fused Deposition Modeling with Polypropylene.” *Materials & Design*, vol. 83, 2015, pp. 768–76. *Crossref*, doi:10.1016/j.matdes.2015.06.053.

Centers for Disease Control and Prevention. “Use masks to slow spread.” *Centers for Disease Control and Prevention* (2020).

Chemical Retrieval on the Web. “Coefficient of Thermal Expansion.” *Polymer Properties Database*, Chemical Retrieval on the Web, polymerdatabase.com/polymer%20physics/Expansion.html. Accessed 16 May 2021.

Edwards, Ed. “What is melt-blown extrusion and how is it used for making masks?” *Thomas Net* (2020).

Gauss, C. et al. “The use of cellulose in bio-derived formulations for 3D/4D printing: A review.” *Composites Part C*: Open Access 4 (2021) 100113.

Hansen, C. M. “Hansen Solubility Parameters: a User's Handbook, Second Edition.” Taylor and Francis. (2007).

Hutten, Irwin M. *Handbook of nonwoven filter media*. Elsevier, 2007. Hutten PerkinElmer. “Dynamic mechanical analysis basics: part 2 thermoplastic transitions and properties.” *Perkin Elmer Technical Notes: Thermal Analysis.* (2007).

Jambeck, J. R., et al. “Plastic Waste Inputs from Land into the Ocean.” *Science*, vol. 347, no. 6223, 2015, pp. 768–71. *Crossref*, doi:10.1126/science.1260352.

Natta, G., et al. “Crystalline Structure of Isotactic Polypropylene.” *Stereoregular Polymers and Stereospecific Polymerizations*, 1967, p. 178. *Crossref*, doi:10.1016/b978-1-4831-9883-5.50028-3.

Patrício Silva, Ana L., et al. “Increased Plastic Pollution Due to COVID-19 Pandemic: Challenges and Recommendations.” *Chemical Engineering Journal*, vol. 405, 2021, p. 126683. *Crossref*, doi:10.1016/j.cej.2020.126683.

Poulakis, J. G., & Papaspyrides, C. D. (1997). "Recycling of polypropylene by the dissolution/reprecipitation technique: I. A model study." *Resources, Conservation and Recycling*, *20*(1), 31–41. https://doi.org/10.1016/s0921-3449(97)01196-8.

Prata, Joana C., et al. "COVID-19 Pandemic Repercussions on the Use and Management of Plastics." *Environmental Science & Technology*, vol. 54, no. 13, 2020, pp. 7760–65. *Crossref*, doi:10.1021/acs.est.0c02178.

Roberson, David. "What Is FFF?: Fused Filament Fabrication Technology for 3D Printing." *Ultimaker.Com*, 6 Jan. 2021, ultimaker.com/learn/what-is-fff-fused-filament-fabrication-technology-for-3d-printing.

Rubinstein, Michael, and Ralph H. Colby. *Polymer Physics (Chemistry)*. 1st ed., Oxford University Press, 2003.

Shahzadi et al. "Advances in lignocellulosic biotechnology: A brief review on lignocellulosic biomass and cellulases." *Advances in Bioscience and Biotechnology* (2014) 5, 246-251.

Silva, A. F., et al. "3D Printing of Polypropylene Using the Fused Filament Fabrication Technique." *Proceedings of the 20th International ESAFORM Conference on Material Forming*, 2017. *Crossref*, doi:10.1063/1.5008040.

SpecialChem SA. "Coefficient of Linear Thermal Expansion (CLTE): Formula & Values." *Omnexus*, 2021, omnexus.specialchem.com/polymer-properties/properties/coefficient-of-linear-thermal-expansion.

Uetsuji et al. "Interfacial adhesion of a grafted polymer on a cellulose surface: a first-principles study." *J Mater Sci* (2021) 56:3589–3599.

USFS Forest Products Laboratory. Purdue University. https://engineering.purdue.edu/nanotrees/what_is_cellulose.shtml

Walker, T. W., Frelka, N., Shen, Z., Chew, A. K., Banick, J., Grey, S., … Huber, G. W. (2020). Recycling of multilayer plastic packaging materials by solvent-targeted recovery and precipitation. *Science Advances*, *6*(47). https://doi.org/10.1126/sciadv.aba7599.

Zhang L. et al. "Natural Fiber-Based Biocomposites." *Green Biocomposites, Green Energy and Technology* (2017).